Analysis of Form Error caused by Thermal Effect in Single Point Diamond Turning Machine

Yu Zhang

Shanghai Engineering Research Center of Ultra-Precision Optical Manufacturing, School of Information Science and Technology, Fudan University, Shanghai, 200438, China;

Abstract. In a single point diamond turning machine, the workpiece inevitably develops an uneven temperature field, leading to surface deformation and subsequently affecting the form accuracy. In this paper, a Twyman-Green interferometer is constructed to measure the thermal deformation of workpiece surfaces. An orthogonal experiment is designed, and the response surface methodology is employed to investigate the effects of spindle speed, cooling water temperature, cooling water flow rate, and air velocity on the thermal deformation of the workpiece. The result indicates that under the conditions of 4000 RPM spindle speed, 23℃ cooling water temperature, 5 L/min cooling water flow rate, and 3 m/s air velocity, the workpiece surface exhibits a protrusion with a higher center and lower periphery, and the amplitude of the protrusion at the workpiece center is 96 nm compared to the edges. The effects of rotational speed, cooling water temperature, and air flow rate on the thermal deformation of the workpiece are more pronounced, while cooling water flow rate has almost no influence. Furthermore, there exists a coupling relationship between the rotational speed and cooling water temperature. Specifically, for every 1% increase in rotational speed, cooling water temperature, and air flow rate, the thermal deformation of the workpiece increases by 1.51%, 2.38%, and 0.34% respectively.

Keywords: Workpiece thermal deformation; FEM; In-situ measurement; Single point diamond turning machine.

1. Introduction

In precision engineering, the machining accuracy is influenced by various factors, including thermal errors, cutter wear, poor geometric accuracy of machine tool components, and fixture errors. Notably, Thermal errors are inherent issues in machine tools, and their formation is quite complex[1]. Thus, the analysis and compensation of thermal errors hold particular importance in the context of ultra-precision machining.

For the research topic of thermal error, scholars have primarily focused on three objects: the motor spindle, the feed system, and the workpiece. Cheng et al. [2] combined thermal images with thermocouple data to model the axial and radial thermal errors of the spindle. They employed a deep learning convolutional neural network for this purpose, achieving a prediction accuracy of approximately 90%-93%. Weng et al. [3] proposed a transient analytical modeling method for the thermal characteristics of machine tools, using after Fourier series and heat conduction partial differential equations to derive the temperature field of the spindle, based on the finite element theory of its calculation of thermal deformation. Zhang et al. [4] proposed a comprehensive positioning error modeling approach for the X-axis of a three-axis CNC machine tool, based on multiple linear regression. This model is intended for compensation and can accurately predict the thermal error of a ball screw at any temperature and position during its temperature rise.

For workpiece, scholars investigated the thermal deformation induced by the friction between the tool and the workpiece. Stefan Schindler et al. [5] utilized MSC.MARC to construct both a local and a global finite element model. The local model employed known cutting parameters to simulate the chip formation process, ultimately yielding boundary conditions such as the heat flow density necessary for the cutting simulation. The global model, on the other hand, accurately calculated the actual position of the tool and was subsequently used in the finite element simulation. Through this process, the researchers were able to obtain the temperature field and the elastic deformation of the workpiece due to thermal expansion. Thermal errors in machine tool components arise from various

reasons, with scholars having addressed nearly all related issues, making the puzzle of thermal error appear complete. However, the thermal deformation of the workpiece due to heat transfer from the spindle remains largely ignored. Jiang et al. [6] conducted nine controlled experiments to investigate the impact of workpiece speed, grinding wheel speed, and feed rate on surface deformation of thin-walled bearings during grinding. Their findings revealed that deformation was primarily induced by machining heat and stress. Specifically, an increase in rotational speed leads to elevated heat flux density within the grinding zone, subsequently enhancing thermal stress on the inner surface of the bearing's inner ring and ultimately causing greater deformation. Existing research on workpiece thermal error often exhibits a tendency to overlook significant aspects while emphasizing minor details. Scholars have predominantly focused on the thermal error induced by cutting heat, neglecting the effects of the spindle, airflow, and cutting fluid on the workpiece. They can generate an uneven temperature distribution within the workpiece, leading to thermal deformation.

In this paper, we combine the results of finite element simulation and interferometer measurements, finding that the workpiece surface deforms, exhibiting a high center and a low periphery, under the combined effect of the spindle, flowing air, and cutting fluid. By analyzing the influence of factors such as rotational speed, cutting fluid temperature, time, and position on the thermal deformation of the workpiece surface, an empirical formula is summarized.

2. System Setup and Configuration

In this paper, Nanoform 700 ultra large frame diamond machining center is used as the object of research. It is equipped with an SP-150 type air bearing spindle. Passages are provided for coolant circulation to maintain thermal stability both in the motor housing and the bearing housing. A passage is also provided for vacuum or air pressure to be supplied through the air bearing and to the face of the spindle for fixturing. which is shown in Fig. 1. As shown in Fig. 2, the workpiece is fixed on the spindle by vacuum adsorption. Evidently, the spindle serves as a continuous heat source for the workpiece, transferring heat to it. The workpiece undergoes forced convection heat exchange on its side and upper surface, respectively, due to the flowing air and cutting fluid. In such a complex temperature field environment, deformation of the workpiece's surface is inevitable.

Figure. 1 Nanoform 700 ultra large frame diamond machining center

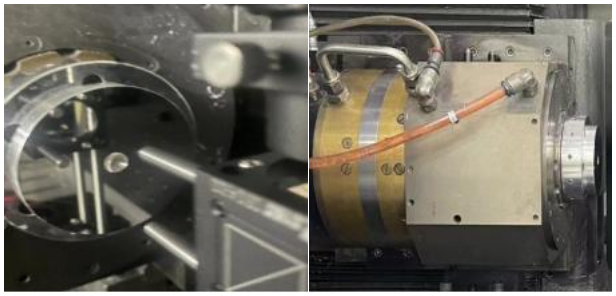

upper surface lateral surface

Figure. 2 The workpiece

During the machining process, heat conduction occurs between the bottom surface of the workpiece and the spindle, while forced convective heat transfer takes place between the lateral surface of the workpiece and the rapidly flowing air. Due to the complete contact between the bottom surface of the workpiece and the spindle, the heat conduction from the spindle to the workpiece is uniform, with consistent conditions at all points on the contact surface. However, forced convective heat transfer between the workpiece and the airflow occurs only on the lateral surface of the workpiece, and the center of the workpiece does not undergo the same heat transfer process. This inevitably leads to a situation where the lateral surface of the workpiece is cooler than the center, resulting in an uneven temperature distribution and subsequent thermal deformation. Furthermore, cutting fluid is often sprayed continuously onto the machined surface of the workpiece during the process. Therefore, in the aforementioned temperature field scenario, the upper surface of the workpiece also experiences forced convective heat transfer with the cutting fluid. The overall situation is illustrated in Fig. 3.

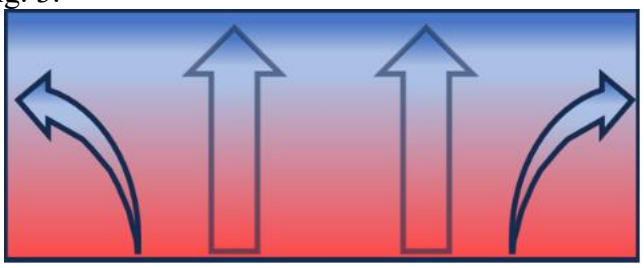

Figure. 3 Heat flow diagram

Finite element simulation can reveal the deformation trend of the workpiece surface for the heretofore unknown problem of surface deformation. Given the cylindrical shape of the workpiece and the uniform action of the heat source, air flow, and cutting fluid on all its surfaces, the deformation of the workpiece's upper surface in this paper is simplified to that on a line segment. Fig. 4 presents the results of finite element simulation, revealing that under the combined influence of the spindle, cutting fluid, and flowing air, the surface of the workpiece experiences deformation, characterized by a higher central region and lower surrounding areas. Compared to the edge of the workpiece, the deformation in the center is on the order of a hundred nanometers. Regarding the temperature field, the distribution within the workpiece is characterized by a high center temperature and lower surrounding temperatures.

Based on the finite element simulation results, a preliminary analysis can be conducted. The workpiece's bottom is continually heated by the spindle, causing an elevation in its temperature. Concurrently, the flowing air on the workpiece's lateral side dissipates some heat from its surface. Consequently, the workpiece develops a temperature field characterized by a hotter interior and a cooler exterior, ultimately leading to surface deformation with a raised center and a lowered periphery.

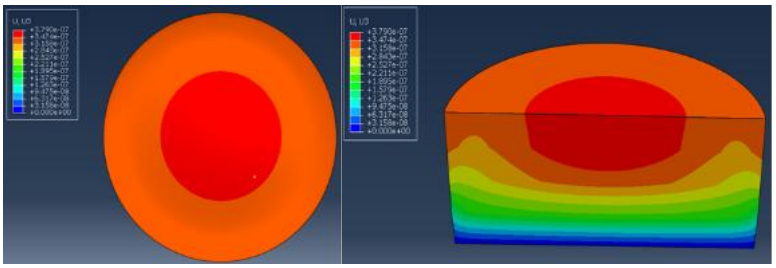

upper surface profile

Figure. 4 Simulation result

3. Exprimental Results

3.1 Workpiece Surface Shape Measurement System

As illustrated in Fig. 5, this paper employs a Twyman Green interferometer [8] to measure the deformation of the workpiece's upper surface during machine tool operation. The optical path diagram of the interferometer is presented in Fig. 6. The interferometer is equipped with a HeNe laser at a wavelength of 632.8 nm as its light source. The beam is expanded by a beam expander into a collimated light, which is then split into two beams by a beam-splitting prism. One beam is reflected by a plane mirror and passes through the beam-splitting prism to enter the camera target surface. The other beam is reflected by the object's surface, follows the original path back, and enters the CCD camera through the beam-splitting prism. Due to the inevitable vibrations of machine tools during operation, solving the phase by the phase shift method is not feasible. Hence, this paper employs the phase recovery method based on Fourier transform [9].

Figure. 5 Interferometer measurement system

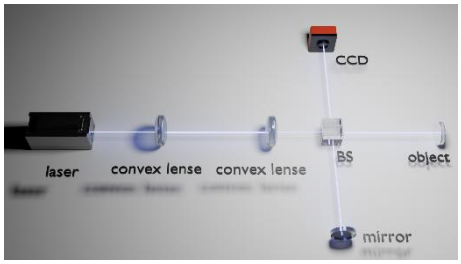

Figure. 6 Optical path diagram

As the systematic error of the interferometer is comprised of background stray light, camera noise, and the interferometer's own error, this paper employs a flat crystal to characterize this error. Fig. 7 shows the interferogram, frequency diagram and phase diagram of the flat crystal, respectively. It is evident that this interferometer possesses a systematic error on the nanometer scale, which is inherent to the system and thus requires subtraction from subsequent measurements. The frequency plot reveals that the zero and positive level spectra are distinct and well-separated, indicating no concern for spectral aliasing or frequency leakage when utilizing the Fourier phase recovery method.

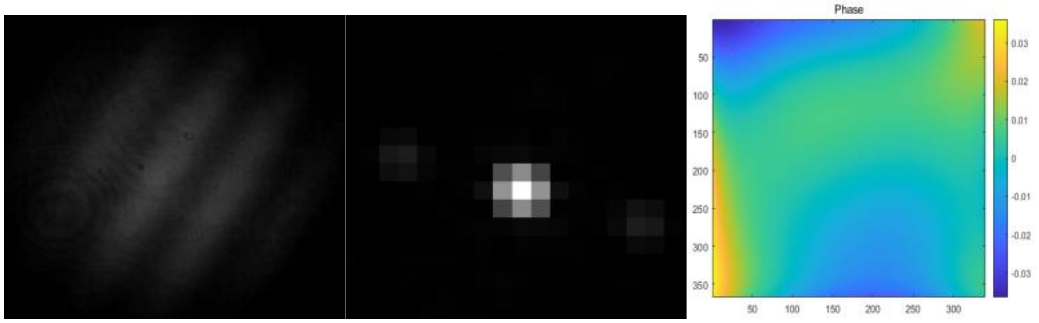

interference figure stroboscopic map phase diagram

Figure. 7 Flat crystal measurement

The experiment aims to address two primary questions: firstly, the specific type of deformation that occurs on the surface of the workpiece due to the combined influence of heat source, air flow, and cutting fluid; and secondly, the factors that are associated with this deformation.

3.2 Analysis of Workpiece Thermal Deformation

Since the thermal deformation of the workpiece surface is a dynamic process, this paper not only analyzes the relationship between thermal deformation and spindle speed, as well as cutting fluid temperature, but also investigates the temporal variation of thermal deformation. This analysis aims to facilitate the realization of dynamic compensation for workpiece thermal errors.

Fig. 8 illustrates the process of workpiece surface deformation under experimental conditions of 4000 RPM spindle speed and 23℃ cutting fluid temperature. The phase diagram reveals that the workpiece surface experiences a deformation characterized by a high center and a low periphery, with the degree of convexity in the middle gradually increasing relative to the periphery. Due to the limitation of experimental conditions, the interferometer does not measure the complete workpiece face shape, but the characteristics of workpiece deformation in the experimental results are consistent with the finite element simulation. Therefore, combining the information of the two, this paper draws the above conclusion.

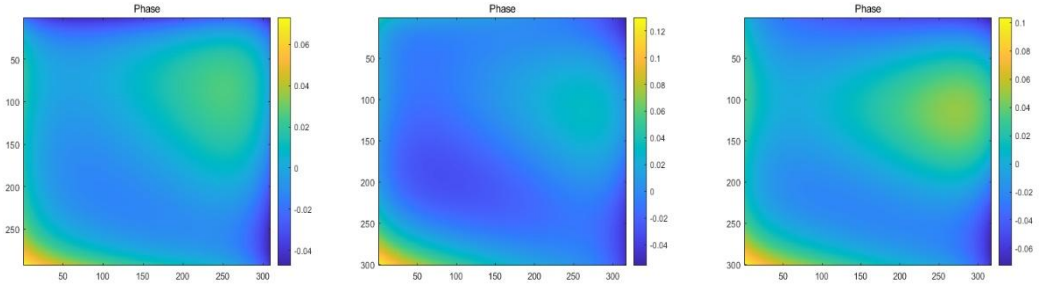

30min 50min 70min

Figure. 8 workpiece thermal deformation phase diagram

In this study, a central composite design method was employed to design the experiments, and the corresponding surface analysis was conducted using Design Expert software. The numerical ranges for the rotational speed, coolant temperature, coolant flow rate, and airflow velocity were set at 2000-5000, 20-23, 5-8, and 3-5, respectively. Table 1 presents the influence degrees of the design parameters and their combinations on the maximum thermal deformation of the workpiece.

Table 1. Significance for each factor

Design parameters	Degree of impact
A-spindle speed	<0.0001
B-coolant temperature	<0.0001
C- coolant flow rate	0.43
D- airflow rate	0.07
AB	0.0009
AC	0.67
AD	0.58
BC	0.67
BD	0.72
CD	0.41

From the table, it is evident that rotational speed, coolant temperature and airflow rate have the most significant influence on thermal deformation, while the impact of coolant flow rate is notably insignificant. Among the interaction terms, only the combination of rotational speed and coolant

temperature exhibits a significant effect. Figure 9 shows the response surface fitting results for factors A and B. When both rotational speed and cooling water temperature reach their maximum values, the workpiece deformation is 130nm. At their minimum values, the deformation is 30nm, with a growth rate of 333.3%.

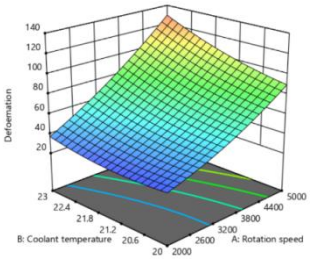

Figuer. 9 AB response surface fit plot

Figure 10 (a) illustrates the growth rate of thermal deformation of the workpiece as the rotational speed increases from 2000 to 5000, representing a 150% increase, under varying cooling water temperatures. Figure 10 (b) depicts the growth rate of thermal deformation of the workpiece with a 15% increase in cooling water temperature under different rotational speed conditions. Under cooling water temperatures of 20, 21, 22, and 23°C, the thermal deformation of the workpiece increases by 1.3%, 1.51%, 1.62%, and 1.63% respectively, for every 1% increase in rotational speed. Similarly, at rotational speeds of 2000, 3000, 4000, and 5000 RPM, the thermal deformation of the workpiece increases by 1.28%, 2.46%, 2.76%, and 3.03% respectively, for every 1% increase in cooling water temperature. Therefore, there exists a coupling relationship between the rotational speed and cooling water temperature. When both factors increase simultaneously, the thermal deformation of the workpiece escalates more significantly. Conversely, when both decrease, the thermal deformation gradually diminishes and tends to stabilize. When the change directions of the two factors are opposite, reducing the cooling water temperature can effectively suppress the thermal deformation induced by an increase in rotational speed.

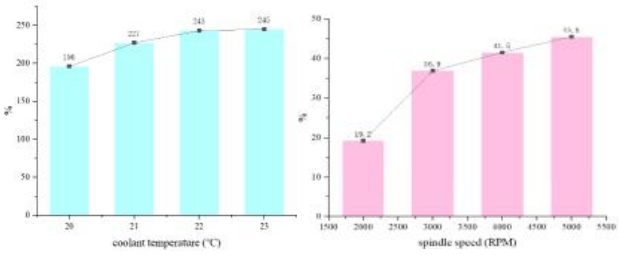

a b

Figure. 10 Rate of thermal deformation growth

In Figure 11, (a) shows the response surface fitting results for factor AD, and (b) shows the response surface fitting results for factor BD. The air velocity does not have a coupling effect with spindle speed and cooling water temperature, and its impact on workpiece thermal deformation is quite limited. When it increases by 66.7%, the thermal deformation of the workpiece only increases by 23.1%. For every 1% increase in air flow rate, the thermal deformation of the workpiece increases by only 0.34%.

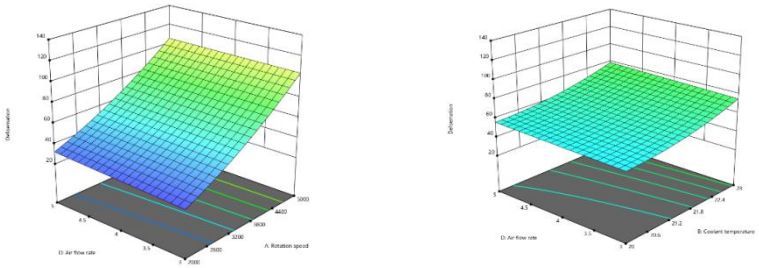

a b

Figure. 11 AD BD response surface fit plot

4. Summary

This paper focuses on Nanoform 700 ultra large frame diamond machining center as the research subject, analyzing the thermal deformation process of the workpiece via finite element simulation and experimentation, while also investigating the effects of spindle speed and cooling water temperature on this deformation. The following conclusions were drawn:

(1) During the machining process, the workpiece is subjected to the combined effects of the spindle, airflow, and cutting fluid, resulting in an uneven temperature distribution within it. This inhomogeneity subsequently induces thermal deformation in the workpiece, characterized by a bulging shape with a higher center and lower periphery, with a deformation magnitude in the order of 100nm.

(2) The effects of rotational speed, cooling water temperature, and airflow rate on the thermal deformation of the workpiece are more pronounced, while the influence of cooling water flow rate on it is negligible. For every 1% increase in rotational speed, cooling water temperature, and airflow rate, the thermal deformation of the workpiece increases by 1.51%, 2.38%, and 0.34%, respectively.

References

[1] G. W. Sun. Effect of Thermal Deformation of Machine Tools on Machining Accuracy. Machine Tools, 1983, 10: 29-30.

[2] Wu C, Xiang S, Xiang W. Spindle thermal error prediction approach based on thermal infrared images: a deep learning method. Journal of Manufacturing Systems 2021, 59: 67–80.

[3] Weng L, Gao W, Zhang D, et al. Analytical modelling of transient thermal characteristics of precision machine tools and real-time active thermal control method. International Journal of Machine Tools and Manufacture, 2023, 186: 104003.

[4] Jun Zhang, Bo Li, Chang Xing Zhou, et al. Positioning error prediction and compensation of ball screw feed drive system with different mounting conditions. Journal of Engineering Manufacture, 2016, 230: 2307-2311.

[5] Stefan Schindler, Marco Zimmermann, Jan C. Aurich. Thermo-elastic deformations of the workpiece when dry turning aluminum alloys - A finite element model to predict thermal effects in the workpiece. CIRP Journal of Manufacturing Science and Technology, 2014, 7: 233–245.

[6] Guo J, Long P, Zhao Y, Xu H, Yang Z, Wang J, Li T, Tang J. Investigation on the deformation and surface quality of a bearing outer ring during grinding processing. Micromachines. 2024; 15: 614.

[7] Sanjib Chatterjee and Y. Pavan Kumar. Measurement of displacement and distance with a polarization phase shifting folded Twyman Green interferometer. Applied Optics, 2015, 54: 9839-9843.

[8] Liu D Yang YY Tian C. Study on phase retrieval from single close fringe pattern with high precision. Chinese Journal of Lasers, 2010, 37:531-536.

[9] Wen long Feng, Zihan Li, Qun ying Gu. Thermally induced positioning error modelling and compensation based on thermal characteristic analysis. International Journal of Machine Tools and Manufacture, 2015, 93: 26-36.